Supporting Information

Color tuning and white light emission by codoping in isostructural homochiral lanthanide metal−organic frameworks

Wenbo Wang,† Ruiying Wang,‡ Yafang Ge,† and Benlai Wu*,†

†College of Chemistry and Molecular Engineering, Zhengzhou University, Zhengzhou 450001, P. R. China

‡School of Chemical Engineering, Henan Vocational College of applied technology, Zhengzhou 450042, P. R. China

*Author for correspondence: Benlai Wu , E-mail: wbl@zzu.edu.cn.

Content

Figure S2. TGA curves of compounds **1**–**4** and the trimetallic doped compound $[(Eu_{0.1388}Gd_{0.6108}Tb_{0.2504})_2(HL)_2(H_2O)_4]\cdot 2Cl\cdot 5H_2O$.

Figure S3. As-synthesized and simulated PXRD patterns of compounds **1**–**4**.

Figure S4. As-synthesized and simulated PXRD patterns of the bimetallic doped compounds $[(Eu_xTb_{1-x})_2(HL)_2(H_2O)_4]\cdot 2Cl\cdot 5H_2O$ (a–i which correspond to the mole fraction of Eu^{3+} being 10.08 mol %, 14.88 mol %, 20.41 mol %, 29.23 mol %, 38.51 mol %, 48.26 mol %, 59.05 mol %, 68.36 mol %, and 79.01 mol %, respectively) and the trimetallic doped compound $[(Eu_{0.1388}Gd_{0.6108}Tb_{0.2504})_2(HL)_2(H_2O)_4]\cdot 2Cl\cdot 5H_2O$.

Figure S5. (a) Coordination environment of Eu^{3+} ions, and (b) binuclear cluster $[Eu_2(COO)_4]$ unit in **2**. Symmetry code: (A) $1 + x$, $1 + y$, z; (B) x, $-1 + y$, z; (C) $1 + x$, y, z.

Figure S6. (a) Coordination environment of Tb^{3+} ions, and (b) binuclear cluster $[Tb_2(COO)_4]$ unit in **3**. Symmetry code: (A) $1 + x$, $1 + y$, z; (B) x, $1 + y$, z; (C) $1 + x$, y, z.

Figure S7. (a) Coordination environment of Dy^{3+} ions, and (b) binuclear cluster $[Dy_2(COO)_4]$ unit in **4**. Symmetry code: (A) x, $1 + y$, z; (B) $1 + x$, $1 + y$, z; (C) $-1 + x$, y, z.

Figure S8. Solid-state excitation spectra of free ligand H_3L (a), **1** (b), **2** (c) and **3** (d) at room temperature.

Figure S9. Solid-state excitation and emission spectra of **4** at room temperature.

Figure S10. Luminescence decay lifetimes of **1** measured at the excitation/emission maxima.

Figure S11. Luminescence decay lifetimes of **2** measured at the excitation/emission maxima.

Figure S12. Luminescence decay lifetimes of **3** measured at the excitation/emission maxima.

Figure S13. Luminescent decay curves [fitting by $I(t) = I_0 + A_1 \exp(t/\tau_1)$] for bimetallic doped $[(Eu_xTb_{1-x})_2(HL)_2(H_2O)_4]\cdot 2Cl\cdot 5H_2O$ (x = 14.88 – 38.51 mol %).

Figure S14. Luminescence decay lifetimes of the trimetallic doped HMOF $[(Eu_{0.1388}Gd_{0.6108}Tb_{0.2504})_2(HL)_2(H_2O)_4]\cdot 2Cl\cdot 5H_2O$ recorded at room temperature with emissions monitored by the $^5D_4 \rightarrow {}^7F_5$ transition at 545 nm and the $^5D_0 \rightarrow {}^7F_2$ transition at 615 nm (λ_{ex} = 370 nm). The red lines are the best fit to the data using a two-exponential function, giving the average values of $\tau_{Tb}{}^{3+}$ = 753.59 μs and $\tau_{Eu}{}^{3+}$= 473.03 μs.

Figure S15. Emission spectra of Tb-HMOF in aqueous solutions of various concentrations of Cr^{3+} under excitation at 352 nm.

Table S1. The Mole Fractions of Eu^{3+} and Tb^{3+} Ions in the Bimetallic Doped Frameworks $[(Eu_xTb_{1-x})_2(HL)_2(H_2O)_4]\cdot 2Cl\cdot 5H_2O$

	a	b	c	d	e	f	g	h	i
Eu^{3+}	0.1008	0.1488	0.2041	0.2923	0.3851	0.4826	0.5905	0.6836	0.7901
Tb^{3+}	0.8992	0.8512	0.7959	0.7077	0.6149	0.5174	0.4095	0.3164	0.2099

Table S2. Selected Bond Lengths (Å) and Angles (°) for 1−4

1			
Gd1−O10	2.310(8)	Gd1−O7	2.386(7)
Gd1−O4A	2.397(7)	Gd1−O5B	2.416(8)
Gd1−O13C	2.434(8)	Gd1−O2	2.439(7)
Gd1−O1	2.453(7)	Gd1−O8	2.469(8)
Gd1−O3A	2.925(8)	Gd2−O3A	2.311(7)
Gd2−O9	2.378(7)	Gd2−O14C	2.392(8)
Gd2−O16	2.400(9)	Gd2−O6B	2.406(8)
Gd2−O11A	2.414(7)	Gd2−O15	2.454(8)
Gd2−O12A	2.475(7)	Gd2−O10	2.913(9)
O10−Gd1−O7	144.3 (3)	O10−Gd1−O4A	123.9(3)
O7−Gd1−O4A	78.3(3)	O10−Gd1−O5B	73.6(3)
O7−Gd1−O5B	142.0(3)	O4A− Gd1−O5B	77.3(3)
O10−Gd1−O13C	82.0(3)	O7−Gd1−O13C	73.1(3)
O4A−Gd1−O13C	82.7(3)	O5B−Gd1−O13C	131.2(3)
O10−Gd1−O2	91.3(3)	O7−Gd1−O2	95.9(3)
O4A−Gd1−O2	126.6(3)	O5B−Gd1−O2	76.3(3)
O13C−Gd1−O2	146.8(3)	O10−Gd1−O1	136.0(3)
O7−Gd1−O1	72.4(3)	O4A−Gd1 –O1	75.3(2)
O5B−Gd1−O1	73.5(3)	O13C−Gd1−O1	142.0(3)
O2−Gd1−O1	53.0(3)	O10−Gd1−O8	77.4(3)

O7−Gd1−O8	71.6(3)	O4A−Gd1−O8	146.2(3)
O5B−Gd1−O8	136.4(3)	O13C−Gd1−O8	74.3(3)
O2−Gd1−O8	72.5(3)	O1−Gd1−O8	108.8(3)
O10−Gd1−O3A	77.4(2)	O7−Gd1−O3A	112.7(2)
O4A−Gd1−O3A	47.4(2)	O5B−Gd1−O3A	68.8(2)
O13C−Gd1−O3A	64.9(3)	O2−Gd1−O3A	145.1(3)
O1−Gd1−O3A	115.9(2)	O8−Gd1−O3A	134.3(3)
O3A−Gd2−O9	124.8(3)	O3A−Gd2−O14C	75.4(3)
O9−Gd2−O14C	75.8(3)	O3A−Gd2−O16	76.6(3)
O9−Gd2−O16	145.4(3)	O14C−Gd2−O16	138.8(3)
O3A−Gd2−O6B	82.3(3)	O9−Gd2−O6B	80.8(3)
O14C−Gd2−O6B	129.0(3)	O16−Gd2−O6B	75.4(3)
O3A−Gd2−O11A	91.0(3)	O9−Gd2−O11A	126.9(3)
O14C−Gd2−O11A	78.1(3)	O16−Gd2−O11A	72.8(3)
O6B−Gd2−O11A	148.2(3)	O3A−Gd2−O15	143.5(3)
O9−Gd2−O15	78.2(3)	O14C−Gd2−O15	141.1(3)
O16−Gd2−O15	71.2(4)	O6B−Gd2−O15	73.6(3)
O11A−Gd2−O15	95.4(3)	O3A−Gd2−O12A	136.9(2)
O9−Gd2−O12A	75.3(2)	O14C−Gd2−O12A	74.2(3)
O16−Gd2−O12A	108.7(3)	O6B−Gd2−O12A	140.8(3)
O11A−Gd2−O12A	53.3(3)	O15−Gd2−O12A	71.5(3)
O3A−Gd2−O10	77.6(2)	O9−Gd2−O10	48.0(2)
O14C−Gd2−O10	67.3(3)	O16−Gd2−O10	133.5(3)
O6B−Gd2−O10	63.3(3)	O11A−Gd2−O10	145.3(3)
O15−Gd2−O10	113.3(3)	O12A−Gd2−O10	116.6(2)
2			
Eu1−O11A	2.313(17)	Eu1−O4B	2.41(2)
Eu1−O14	2.41(3)	Eu11−O5C	2.425(18)
Eu1−O1	2.46(2)	Eu1−O7	2.47(2)

Eu1−O2	2.472(15)	Eu1−O8	2.51(3)
Eu1−O3B	2.789(16)	Eu2−O3B	2.351(16)
Eu2−O12A	2.39(3)	Eu2−O16	2.413(19)
Eu2−O15	2.41(2)	Eu2−O10C	2.417(16)
Eu2−O13	2.43(2)	Eu2−O6C	2.44(2)
Eu2−O9C	2.46(2)	Eu2−O11A	3.023(17)
O11A−Eu1−O4B	128.3(7)	O11A−Eu1−O14	80.6(8)
O4B−Eu1−O14	81.5(9)	O11A−Eu1−O5C	77.6(6)
O4B−Eu1−O5C	76.1(7)	O14−Eu1−O5C	127.6(7)
O11A−Eu1−O1	137.2(7)	O4B−Eu1−O1	74.9(8)
O14−Eu1−O1	142.1(8)	O5C−Eu1−O1	74.7(7)
O11A−Eu1−O7	138.2(7)	O4B−Eu1−O7	80.7(7)
O14−Eu1−O7	74.5(8)	O5C−Eu1−O7	143.9(7)
O1−Eu1−O7	72.8(7)	O11A−Eu1−O2	89.4(5)
O4B−Eu1−O2	124.8(7)	O14−Eu1−O2	151.1(7)
O5C−Eu1−O2	75.4(6)	O1−Eu1−O2	52.4(6)
O7−Eu1−O2	96.5(7)	O11A−Eu1−O8	72.5(10)
O4B−Eu1−O8	145.8(10)	O14−Eu1−O8	75.6(9)
O5C−Eu1−O8	138.2(9)	O1−Eu1−O8	109.1(9)
O7−Eu1−O8	69.0(10)	O2−Eu1−O8	75.6(7)
O11A−Eu1−O3B	80.3(5)	O4B−Eu1−O3B	48.6(6)
O14−Eu1−O3B	62.1(7)	O5C−Eu1−O3B	67.5(5)
O1−Eu1−O3B	117.0(6)	O7−Eu1−O3B	115.0(6)
O2−Eu1−O3B	142.8(5)	O8−Eu1−O3B	132.7(8)
O3B−Eu2−O12A	120.4(8)	O3B−Eu2−O16	148.4(6)
O12A−Eu2−O16	77.6(8)	O3B−Eu2−O15	80.4(8)
O12A−Eu2−O15	146.1(9)	O16−Eu2−O15	73.0(8)
O3B−Eu2−O10C	94.9(5)	O12A−Eu2−O10C	127.1(8)
O16−Eu2−O10C	92.4(6)	O15−Eu2−O10C	71.2(9)

O3B−Eu2−O13	71.0(6)	O12A−Eu2−O13	77.3(8)
O16−Eu2−O13	140.6(7)	O15−Eu2−O13	136.6(8)
O10C−Eu2−O13	79.3(6)	O3B−Eu2−O6C	84.3(6)
O12−Eu2−O6C	82.4(9)	O16−Eu2−O6C	72.0(7)
O15−Eu2−O6C	72.8(10)	O10C−Eu2−O6C	143.6(8)
O13−Eu2−O6C	133.2(8)	O3B−Eu2−O9C	136.1(7)
O12A−Eu2−O9C	74.1(9)	O16−Eu2−O9C	71.0(7)
O15−Eu2−O9C	110.8(10)	O10C−Eu2−O9C	53.9(7)
O13−Eu2−O9C	73.1(8)	O6C−Eu2−O9C	139.5(7)
		3	
Tb1−O10A	2.297(18)	Tb1−O1	2.348(14)
Tb1−O13	2.38(2)	Tb1−O6A	2.380(19)
Tb1−O8	2.392(19)	Tb1−O3B	2.403(19)
Tb1−O7	2.43(2)	Tb1−O4B	2.485(19)
Tb2−O2	2.285(17)	Tb2−O16	2.387(18)
Tb2−O9A	2.397(14)	Tb2−O14	2.41(2)
Tb2−O11C	2.42(2)	Tb2−O12C	2.430(18)
Tb2−O5A	2.44(2)	Tb2−O15	2.47(2)
O10A−Tb1−O1	124.2(6)	O10A−Tb1−O13	83.0(7)
O1−Tb1−O13	79.5(6)	O10A−Tb1−O6A	72.7(6)
O1−Tb1−O6A	79.5(6)	O13−Tb1−O6A	130.2(7)
O10A−Tb1−O8	80.0(7)	O1−Tb1−O8	141.8(7)
O13−Tb1−O8	74.5(8)	O6A−Tb1−O8	138.6(8)
O10A−Tb1−O3B	90.3(7)	O1−Tb1−O3B	129.0(6)
O13−Tb1−O3B	147.3(8)	O6A−Tb1−O3B	76.8(8)
O8−Tb1−O3B	72.8(9)	O10A−Tb1−O7	145.8(6)
O1−Tb1−O7	76.2(6)	O13−Tb1−O7	73.7(7)
O6A−Tb1−O7	141.4(7)	O8−Tb1−O7	70.0(8)
O3B−Tb1−O7	96.0(8)	O10A−Tb1−O4B	134.7(6)

O1−Tb1−O4B	77.0(6)	O13−Tb1−O4B	142.3(7)
O6A−Tb1−O4B	73.4(6)	O8−Tb1−O4B	107.9(7)
O3B−Tb1−O4B	53.1(7)	O7−Tb1−O4B	72.3(7)
O2−Tb2−O16	141.4(6)	O2−Tb2−O9A	124.2(6)
O16−Tb2−O9A	81.4(6)	O2−Tb2−O14	76.6(6)
O16−Tb2−O14	142.0(7)	O9A−Tb2−O14	72.8(6)
O2−Tb2−O11C	90.6(6)	O16−Tb2−O11C	96.1(7)
O9A−Tb2−O11C	125.7(6)	O14−Tb2−O11C	78.0(8)
O2−Tb2−O12C	137.6(6)	O16−Tb2−O12C	72.1(7)
O9A−Tb2−O12C	74.8(5)	O14−Tb2−O12C	74.5(7)
O11C−Tb2−O12C	53.5(6)	O2−Tb2−O5A	81.9(7)
O16−Tb2−O5A	73.0(7)	OA−Tb2−O5A	82.2(6)
O14−Tb2−O5A	128.4(7)	O11C−Tb2−O5A	149.0(7)
O12C−Tb2−O5A	140.5(7)	O2−Tb2−O15	73.5(7)
O16−Tb2−O15	72.1(8)	O9A−Tb2−O15	149.3(7)
O14−Tb2−O15	137.9(8)	O11C−Tb2−O15	73.5(8)
O12C−Tb2−O15	110.2(7)	O5A−Tb2−O15	75.5(7)
	4		
Dy1−O10	2.298(18)	Dy1−O7	2.381(18)
Dy1−O4A	2.40(2)	Dy1−O13B	2.399(18)
Dy1−O5C	2.41(2)	Dy1−O2	2.428(12)
Dy1−O1	2.44(2)	Dy1−O8	2.455(19)
Dy2−O3A	2.270(17)	Dy2−O9	2.34(2)
Dy2−O14B	2.36(2)	Dy2−O16	2.37(2)
Dy2−O11A	2.392(12)	Dy2−O15	2.406(18)
Dy2−O6C	2.41(2)	Dy2−O12A	2.48(2)
O10−Dy1−O7	144.9(6)	O10−Dy1−O4A	122.1(7)
O7−Dy1−O4A	79.9(7)	O10−Dy1−O13B	83.6(6)
O7−Dy1−O13B	73.4(6)	O4A−Dy1−O13B	79.5(7)

O10−Dy1−O5C	72.8(7)	O7−Dy1−O5C	142.3(7)
O4A−Dy1−O5C	75.8(8)	O13B−Dy1−O5C	128.5(7)
O10−Dy1−O2	88.1(5)	O7−Dy1−O2	100.5(5)
O4A−Dy1−O2	125.8(6)	O13B−Dy1−O2	153.2(5)
O5C−Dy1−O2	72.2(6)	O10−Dy1−O1	135.6(7)
O7−Dy1−O1	72.6(7)	O4A−Dy1−O1	75.5(7)
O13B−Dy1−O1	140.6(6)	O5C−Dy1−O1	73.5(7)
O2−Dy1−O1	54.2(5)	O10−Dy1−O8	77.9(7)
O7−Dy1−O8	71.5(7)	O4A−Dy1−O8	147.3(7)
O13B−Dy1−O8	77.4(6)	O5C−Dy1−O8	136.8(7)
O2−Dy1−O8	76.0(6)	O1−Dy1−O8	109.6(7)
O3A−Dy2−O9	125.7(7)	O3A−Dy2−O14B	77.2(7)
O9−Dy2−O14B	76.5(7)	O3A−Dy2−O16	75.3(7)
O9−Dy2−O16	143.9(7)	O14B−Dy2−O16	139.6(7)
O3A−Dy2−O11A	92.0(5)	O9−Dy2−O11A	129.9(6)
O14−Dy2−O11A	82.5(6)	O16−Dy2−O11A	69.5(6)
O3A−Dy2−O15	142.3(6)	O9−Dy2−O15	77.9(7)
O14B−Dy2−O15	140.4(7)	O16−Dy2−O15	70.8(7)
O11A−Dy2−O15	91.4(6)	O3A−Dy2−O6C	80.1(7)
O9−Dy2−O6C	81.5(7)	O14B−Dy2−O6C	129.5(7)
O16−Dy2−O6C	73.5(7)	O11A−Dy2−O6C	142.9(5)
O15−Dy2−O6C	74.9(7)	O3A−Dy2−O12A	137.2(6)
O9−Dy2−O12A	76.8(7)	O14B−Dy2−O12	73.9(7)
O16−Dy2−O12A	108.6(7)	O11A−Dy2−O12 A	53.7(6)
O15−Dy2−O12A	71.2(7)	O6C−Dy2−O12A	142.7(7)

Symmetry codes: (A) x, $1 + y$, z; (B) $-1 + x$, y, z; (C) $1 + x$, $1 + y$, z for **1**. (A) $1 + x$, $1 + y$, z; (B) x, $-1 + y$, z; (C) $1 + x$, y, z for **2**. (A) $1 + x$, $1 + y$, z; (B) x, $1 + y$, z; (C) $1 + x$, y, z for **3**. (A) x, $1 + y$, z; (B) $1 + x$, $1 + y$, z; (C) $-1 + x$, y, z for **4**.

Table S3. The Lifetime for Tb^{3+} and Eu^{3+} Ions Ions in the Bimetallic Doped compounds $[(Eu_xTb_{1-x})_2(HL)_2(H_2O)_4]\cdot 2Cl\cdot 5H_2O$ Monitored by the $^5D_4 \rightarrow {}^7F_5$ Transition at 545 nm and the $^5D_0 \rightarrow {}^7F_2$ Transition at 615 nm (λ_{ex} = 370 nm)

x	0	0.1488	0.2041	0.2913	0.3851
$\tau_{Tb}{}^{3+}$ (μs)	826.26	672.96	655.00	577.62	440.67
$\tau_{Eu}{}^{3+}$ (μs)	0	317.23	329.17	358.89	283.46

Table S4. The CIE Coordinates of the Emissions of the Eu/Tb Doped HMOFs $[(Eu_xTb_{1-x})_2(HL)_2(H_2O)_4]\cdot 2Cl\cdot 5H_2O$ upon Excitation at 370 nm.

The mole fractions of Eu^{3+} and Eu^{3+} in the samples	CIE coordinates
$Eu_{0.1008}Tb_{0.8992}$	(0.325, 0.468)
$Eu_{0.1488}Tb_{0.8512}$	(0.333, 0.443)
$Eu_{0.2041}Tb_{0.7959}$	(0.368, 0.401)
$Eu_{0.2923}Tb_{0.7077}$	(0.406, 0.360)
$Eu_{0.3851}Tb_{0.6149}$	(0.410, 0.330)
$Eu_{0.4826}Tb_{0.5174}$	(0.432, 0.313)
$Eu_{0.5905}Tb_{0.4095}$	(0.449, 0.292)
$Eu_{0.6836}Tb_{0.3164}$	(0.460, 0.290)
$Eu_{0.7901}Tb_{0.2099}$	(0.470, 0.287)

Table S5. The CIE Coordinates of the Emissions of the Trimetallic Doped HMOF $[(Eu_{0.1388}Gd_{0.6108}Tb_{0.2504})_2(HL)_2(H_2O)_4]\cdot 2Cl\cdot 5H_2O$ upon Excitation from 310 to 370 nm

Excitation wavelength (nm)	CIE coordinates
310	(0.375, 0.501)
320	(0.363, 0.478)
330	(0.352, 0.432)
340	(0.341, 0.380)
350	(0.324, 0.347)
355	(0.317, 0.331)
360	(0.300, 0.315)
370	(0.285, 0.298)

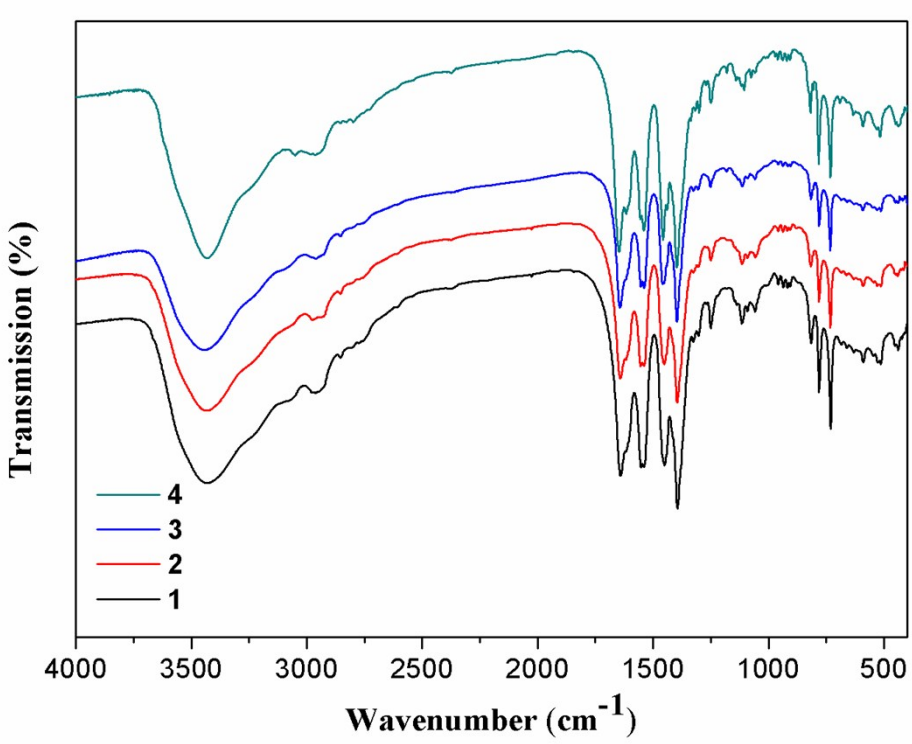

Figure S1. The FT-IR spectra of **1**–**4**.

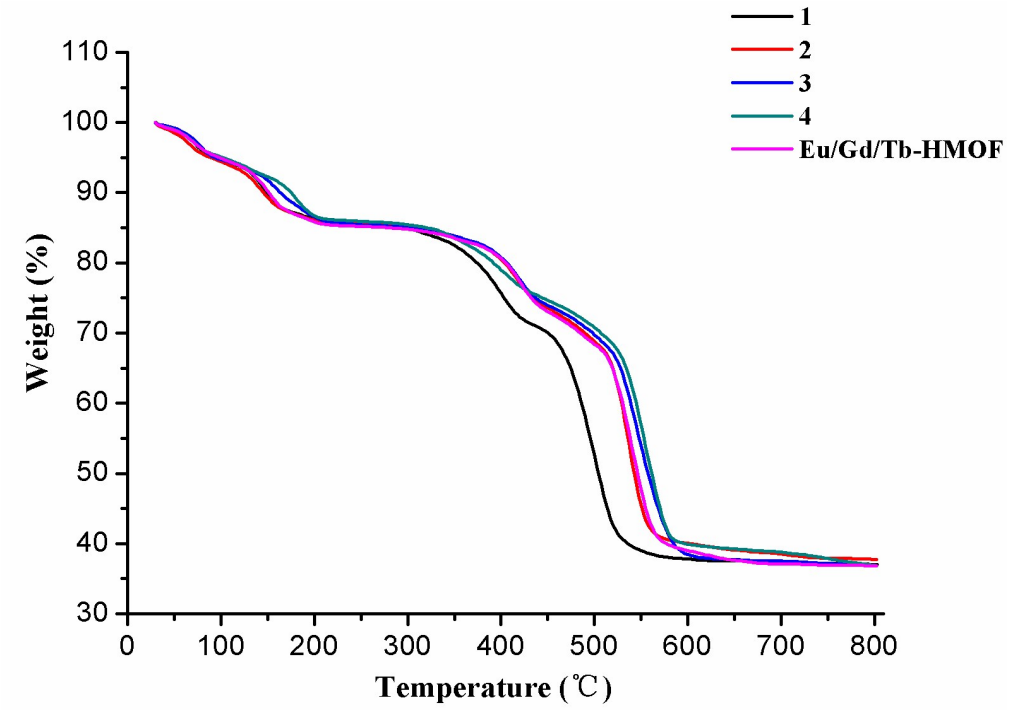

Figure S2. TGA curves of compounds **1**–**4** and the trimetallic doped compound $[(Eu_{0.1388}Gd_{0.6108}Tb_{0.2504})_2(HL)_2(H_2O)_4]\cdot 2Cl\cdot 5H_2O$.

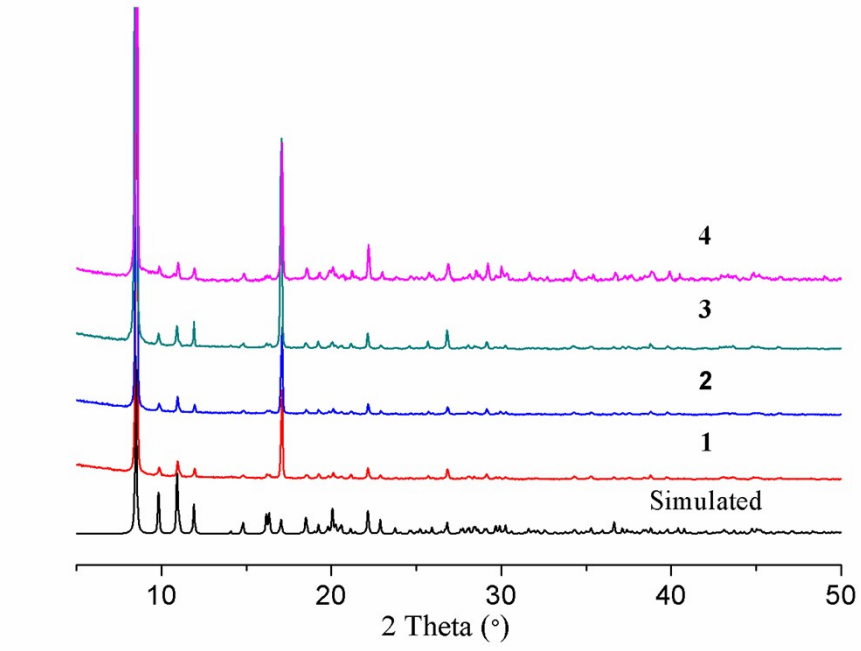

Figure S3. As-synthesized and simulated PXRD patterns of compounds **1**–**4**.

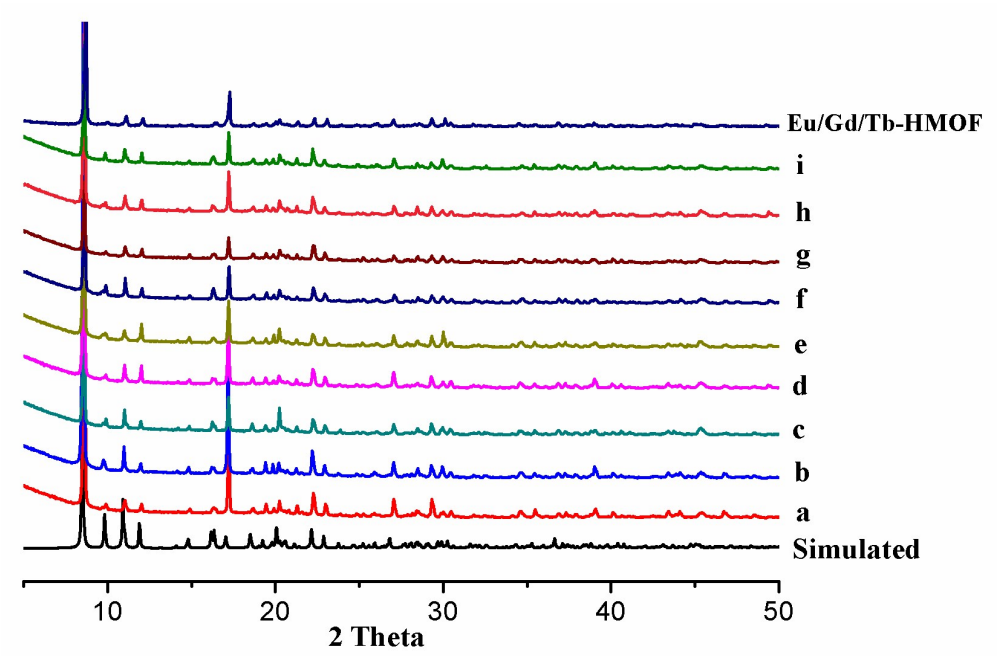

Figure S4. As-synthesized and simulated PXRD patterns of the bimetallic doped compounds $[(Eu_xTb_{1-x})_2(HL)_2(H_2O)_4]\cdot 2Cl\cdot 5H_2O$ (a–i which correspond to the mole fraction of Eu^{3+} being 10.08 mol %, 14.88 mol %, 20.41 mol %, 29.23 mol %, 38.51 mol %, 48.26 mol %, 59.05 mol %, 68.36 mol %, and 79.01 mol %, respectively) and the trimetallic doped compound $[(Eu_{0.1388}Gd_{0.6108}Tb_{0.2504})_2(HL)_2(H_2O)_4]\cdot 2Cl\cdot 5H_2O$.

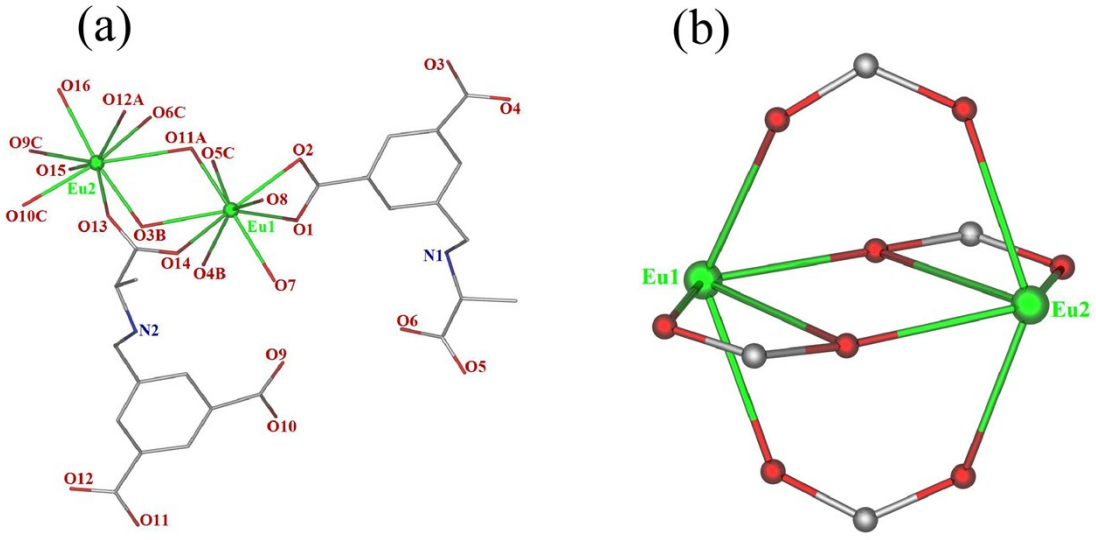

Figure S5. (a) Coordination environment of Eu^{3+} ions, and (b) binuclear cluster $[Eu_2(COO)_4]$ unit in **2**. Symmetry code: (A) $1 + x$, $1 + y$, z; (B) x, $-1 + y$, z; (C) $1 + x$, y, z.

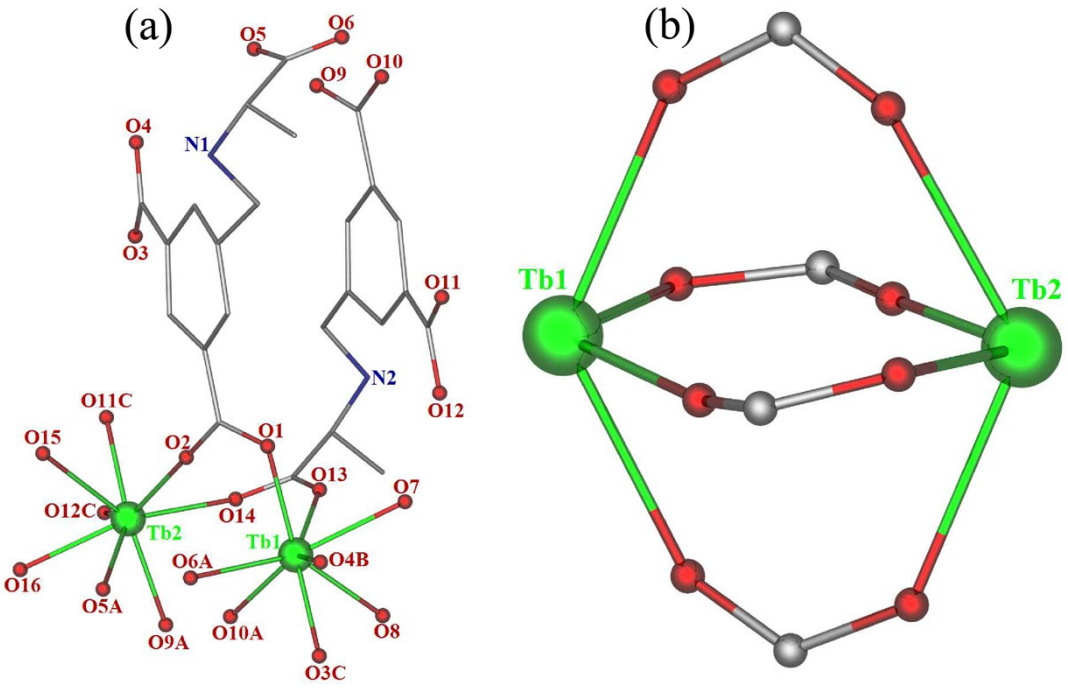

Figure S6. (a) Coordination environment of Tb^{3+} ions, and (b) binuclear cluster $[Tb_2(COO)_4]$ unit in **3**. Symmetry code: (A) $1 + x$, $1 + y$, z; (B) x, $1 + y$, z; (C) $1 + x$, y, z.

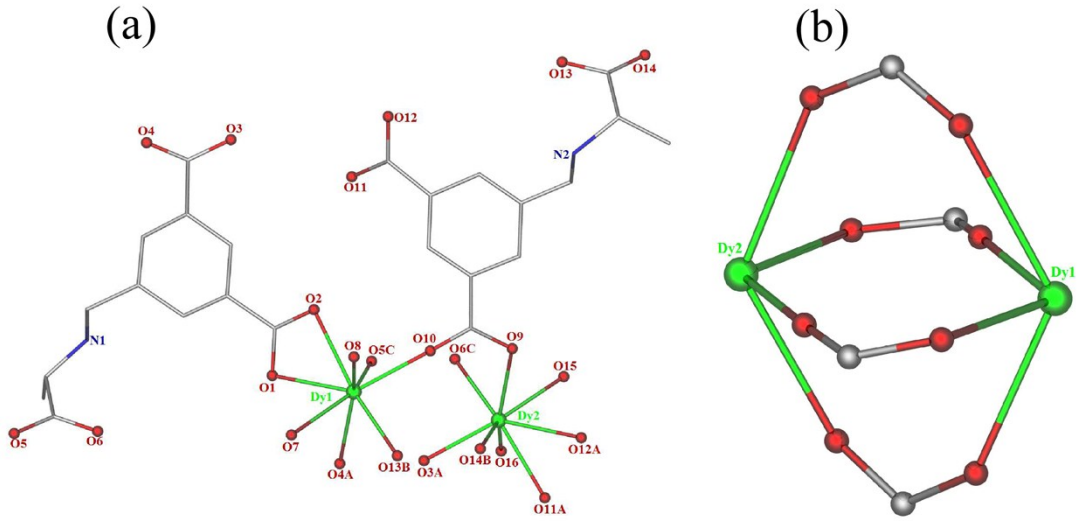

Figure S7. (a) Coordination environment of Dy^{3+} ions, and (b) binuclear cluster $[Dy_2(COO)_4]$ unit in **4**. Symmetry code: (A) x, $1 + y$, z; (B) $1 + x$, $1 + y$, z; (C) $-1 + x$, y, z.

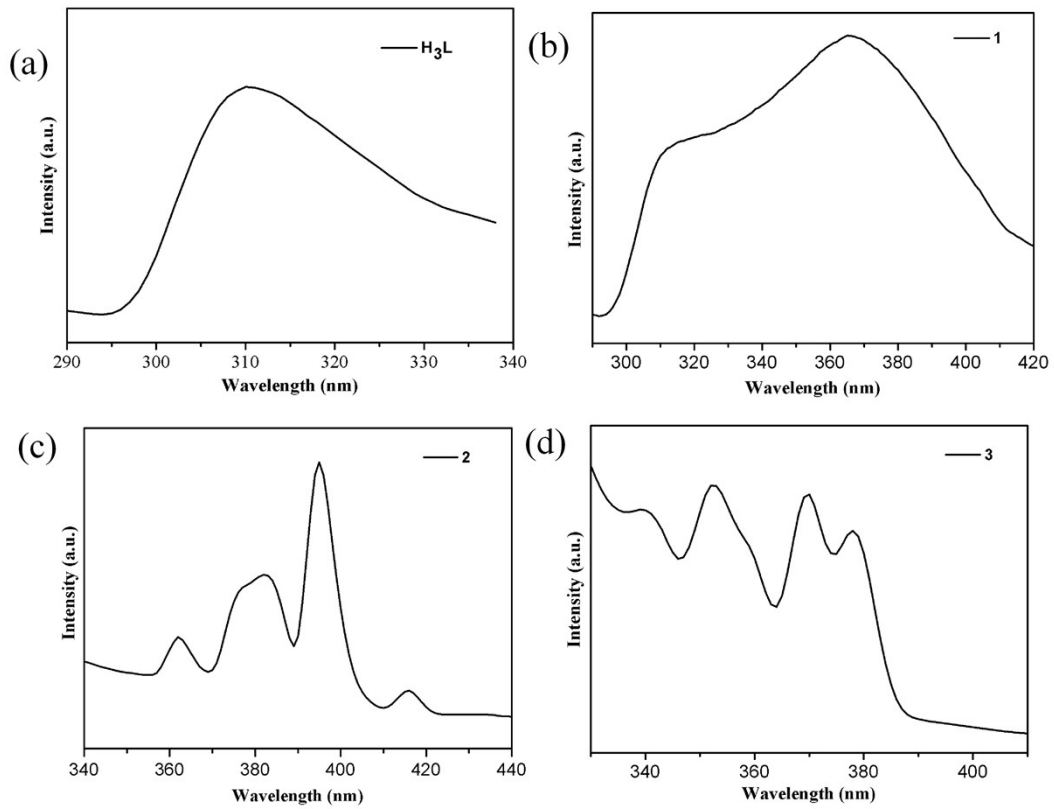

Figure S8. Solid-state excitation spectra of free ligand H_3L (a), **1** (b), **2** (c) and **3** (d) at room temperature.

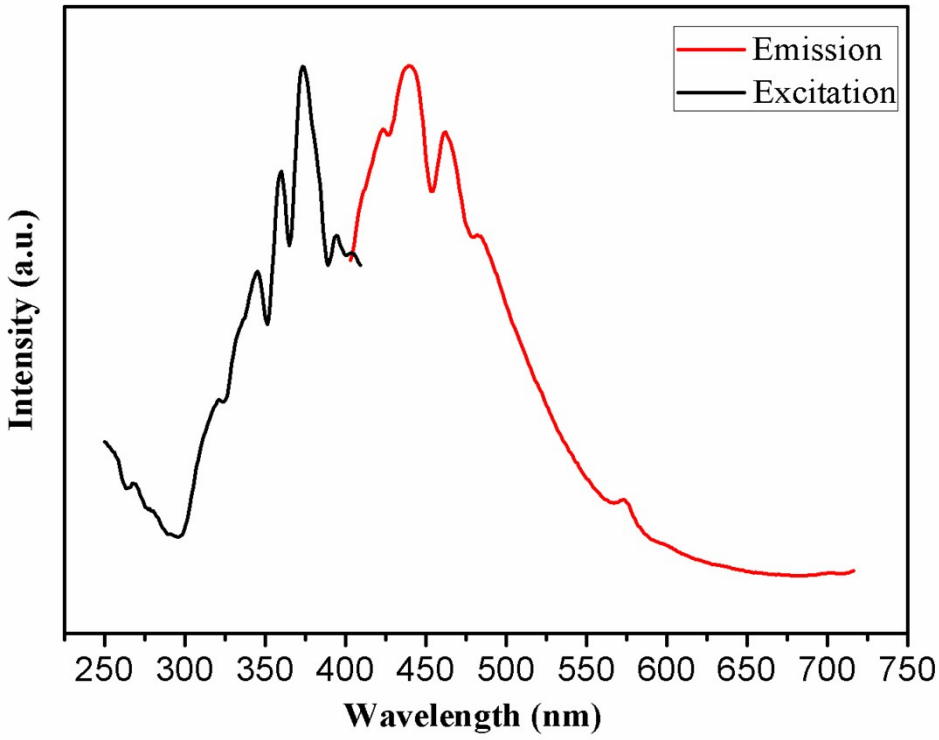

Figure S9. Solid-state excitation and emission spectra of **4** at room temperature.

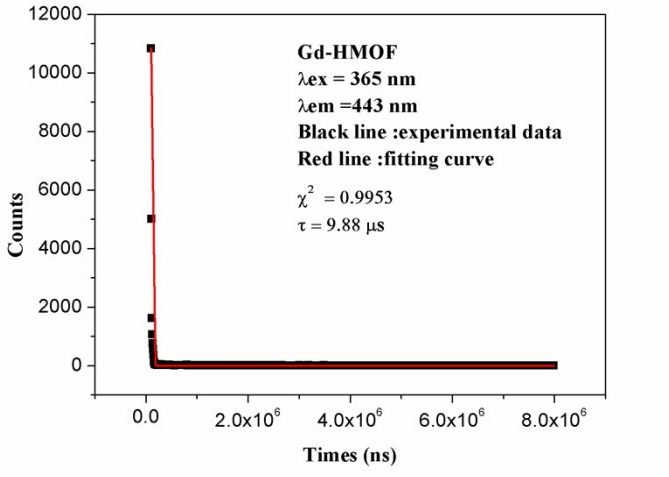

Figure S10. Luminescence decay lifetimes of **1** measured at the excitation/emission maxima.

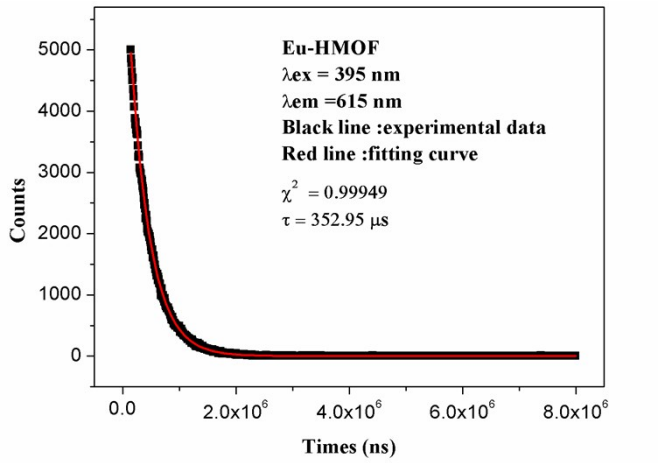

Figure S11. Luminescence decay lifetimes of **2** measured at the excitation/emission maxima.

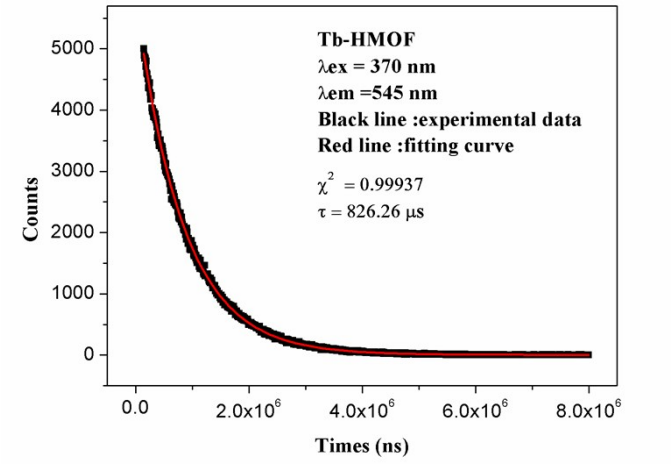

Figure S12. Luminescence decay lifetimes of **3** measured at the excitation/emission maxima.

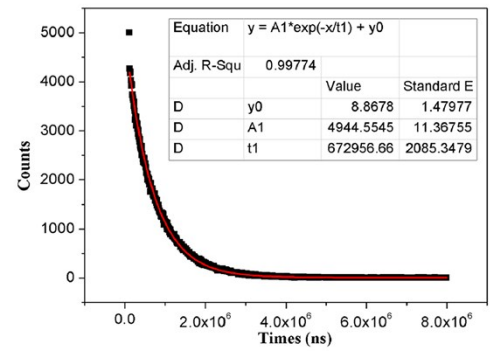

$Eu_{0.1488}Tb_{0.8512}$-HMOF

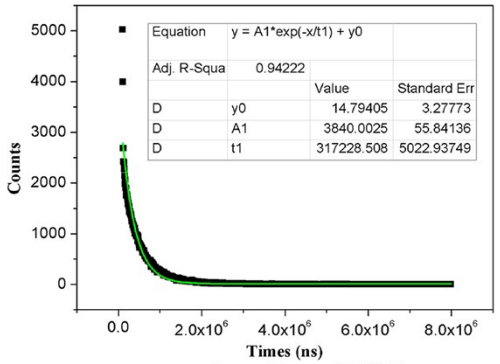

$Eu_{0.1488}Tb_{0.8512}$-HMOF

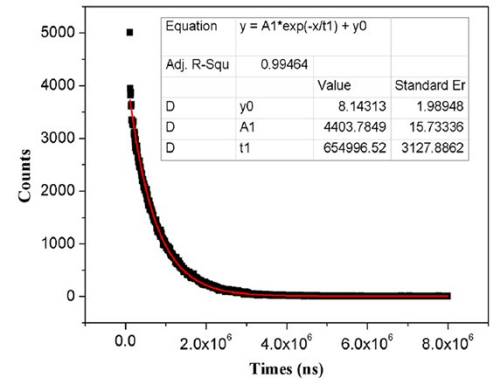

$Eu_{0.2041}Tb_{0.7959}$-HMOF

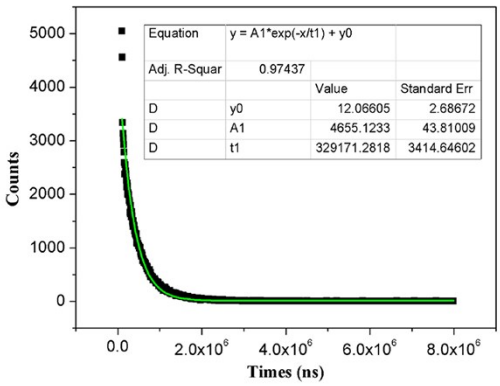

$Eu_{0.2041}Tb_{0.7959}$-HMOF

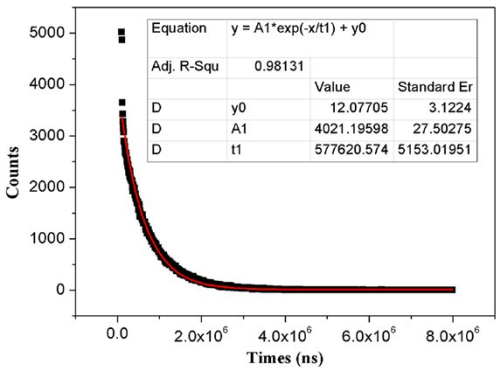

$Eu_{0.2923}Tb_{0.7077}$-HMOF

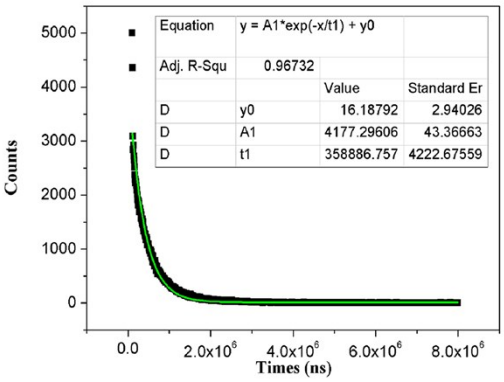

$Eu_{0.2923}Tb_{0.7077}$-HMOF

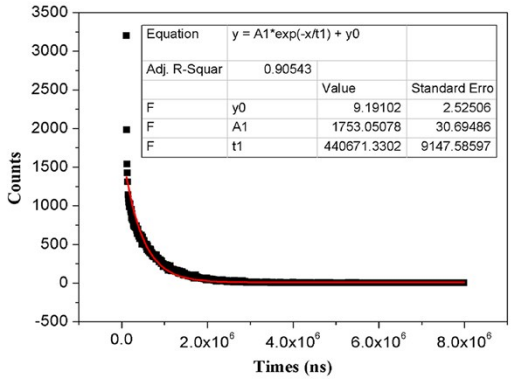

$Eu_{0.3851}Tb_{0.6149}$-HMOF

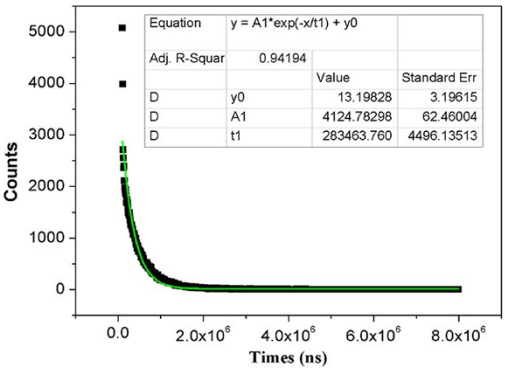

$Eu_{0.3851}Tb_{0.6149}$-HMOF

Figure S13. Luminescent decay curves [fitting by $I(t) = I_0 + A_1 \exp(t/\tau_1)$] for bimetallic doped $[(Eu_xTb_{1-x})_2(HL)_2(H_2O)_4]\cdot 2Cl\cdot 5H_2O$ (x = 14.88 – 38.51 mol %).

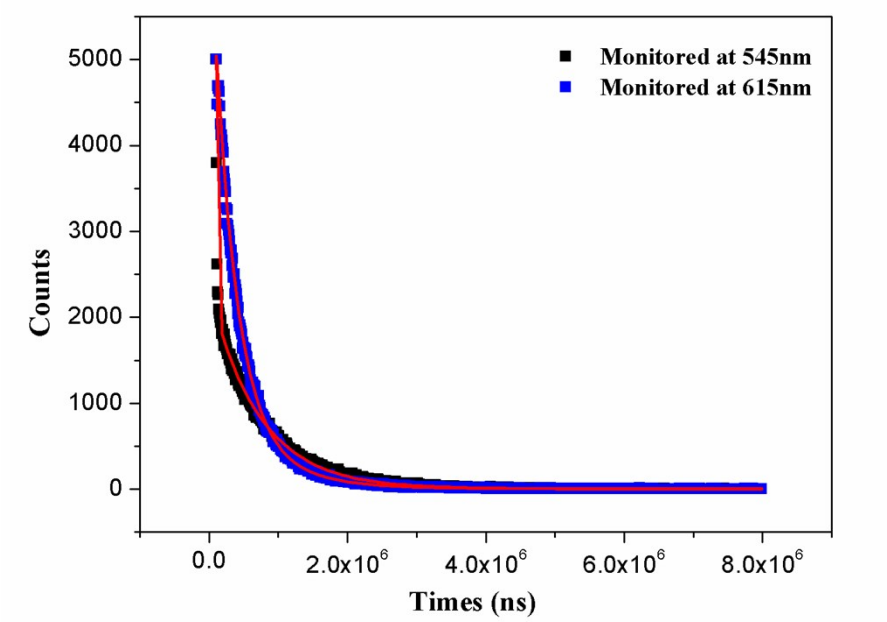

Figure S14. Luminescence decay lifetimes of the trimetallic doped HMOF $[(Eu_{0.1388}Gd_{0.6108}Tb_{0.2504})_2(HL)_2(H_2O)_4]\cdot 2Cl\cdot 5H_2O$ recorded at room temperature with emissions monitored by the $^5D_4 \rightarrow {}^7F_5$ transition at 545 nm and the $^5D_0 \rightarrow {}^7F_2$ transition at 615 nm (λ_{ex} = 370 nm). The red lines are the best fit to the data using a two-exponential function, giving the average values of τ_{Tb}^{3+} = 753.59 μs and τ_{Eu}^{3+}= 473.03 μs.

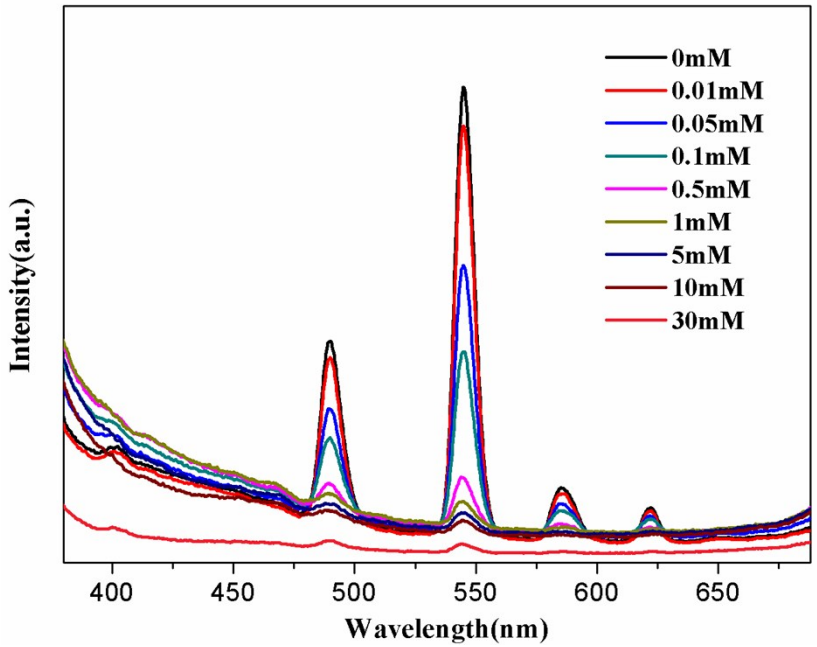

Figure S15. Emission spectra of Tb-HMOF in aqueous solutions of various concentrations of Cr^{3+} under excitation at 352 nm.